


Research Article

Multi-State Reliability Analysis Based on General Wiener Degradation Process and Random Shock

Huibing Hao ^{1,2} and Chunping Li ²

¹School of Management, Suqian University, Suqian 223800, China

²Department of Mathematics and Statistics, Hubei Engineering University, Xiaogan 432100, China

Correspondence should be addressed to Chunping Li; lichunping315@163.com

Received 2 August 2022; Revised 15 September 2022; Accepted 24 September 2022; Published 26 October 2022

Academic Editor: Fabrizio Scozzese

Copyright © 2022 Huibing Hao and Chunping Li. This is an open access article distributed under the Creative Commons Attribution License, which permits unrestricted use, distribution, and reproduction in any medium, provided the original work is properly cited.

A multi-state reliability analysis model suffering from a dependent competing failure process is developed in this study, where the soft failure is described by general nonlinearity random effect. Wiener degradation process with measurement error and the hard failure is caused by random shock. Considering that the shock process not only may cause abrupt damage but also can accelerate degradation, there are some correlations between soft failure and hard failure. Based on the proposed new model, the multi-state functions are obtained under the cumulative shock model and the extreme shock model, and the system state probabilities are given under the different degradation state points. The fatigue cracks growth data example and MEMS oscillator example are given to demonstrate the proposed new model. At last, some sensitivity analyses are given to illustrate the influence of parameters on the state probability and the system reliability.

1. Introduction

In many actual engineering environments, system reliability is not only related to the service time but also related to the system state, such as humidity, wear, random shock, erosion, and vibration, any of which can lead to system degradation. Considering the impact of different degrees of degradation, the systems may exist in lots of different medial states within the life cycle, and different degradation states can perform various distinctive tasks. Therefore, the multi-state reliability modeling and calculation of the complex degradation system can provide an effective technical approach to the reliability theory.

The concept of multi-state reliability is defined as a complex system with a series of performance levels in its life cycle, including in perfect function state, intermediate unction state, and complete failure state [1]. Many study methods are used to deal with multi-state reliability modeling, such as the multi-state RBD method [2], Markov process method [3], semi-Markov process method [4], and some other related research about the multi-state degradation reliability modeling can be found in Refs [5–9].

In real circumstances, except for performance degradation, the system components are often subject to different random shocks. We know that those random shocks may bring a faster degradation rate, resulting in the system's performance degradation level from one state to another. There are some papers focusing on the random shock to the multi-state reliability problem. For example, Li and Pham [10] developed a generalized condition-based maintenance model subject to degradation and shock, Eryilmaz [11] studied the assessment of the multi-state shock model; Segovia and Labeau [12] studied a multi-state reliability model subject to the wear-out process and shock process; Li and Pham [13] studied a multi-state failure processes reliability model suffering from the degradation and shocks. Lin et al. [14] studied the assessment of the multi-state system under different random shocks; Pham et al. [15] presented a model for predicting the availability and mean a lifetime of multistage degraded systems with partial repairs.

In practice engineering applications, because the shock process not only may cause abrupt damage but also can accelerate the degradation, there are some correlations between degradation failure and shock failure. Some multi-state

reliability analyses for the system subject to the dependent competing failure process (DCFP) model have been studied [16–26], such as Wang et al. [23] constructed the DCFP model by using multi-state system reliability theory and line degradation path; Jiang et al. [24] constructed a multi-state reliability analysis for DCFP with line degradation process by using delay time theory; Li et al. [25] and Wang et al. [26] constructed reliability model for multi-state systems by using shock model and normal distribution model.

Considering that the nonlinearity, uncertainty, and individual differences exist extensively in the practice degradation process, see Refs [27–30]. Therefore, some multi-state complex degradation system reliability assessment models suffering from the DCFP model are proposed in this paper, where the degradation failure process is described by a general nonlinear random effect. Wiener degradation process with measurement errors and the abrupt failure process is described by two different shock models. Based on the proposed new model, the multi-state reliability functions are given, and the system state probabilities are obtained under the different degradation state points. At last, the fatigue cracks growth data example and MEMS oscillator example are given to demonstrate the proposed new model.

2. Model Descriptions

As shown in Figures 1 and 2, a complex system may fail due to the DCFP: soft failure caused by continuous degradation such as wear, corrosion, humidity, wear, and erosion, and hard failure caused by the stress from the shock process, such as random shock, vibration, and fracture. In this paper, the soft failure process can be described as nature degradation process and the additional abrupt increment by the shock loads; the soft failure occurs when the total degradation $X_s(t)$ is above its threshold level H , where the total degradation volume contains the nature degradation and additional abrupt increment by the shock load. The hard failure can be affected by the same shock process, and hard failure happens when the shock magnitude exceeds its threshold level D . Let Y_i and W_i ($i = 1, 2, 3, \dots$) denote the abrupt damage size and the magnitude of i th shock load, respectively. These two types of failure processes are dependent because they suffer the same shock. In this paper, the cumulative shock model and the extreme shock model are used, and each shock can bring a change to the system state.

3. System Reliability Assessment Based on the Multi-State Theory

3.1. Shocking Process Analysis. As we know, shock is a significant reason for system failure. In practical running environments, many factors could bring all kinds of shocks to systems, and those factors may come from the external environment, such as sudden or unexpected usage loads. Suppose that the arrives of random shocks follows a Poisson distribution with parameter λ , then we have

$$P\{N(t) = i\} = \frac{(\lambda t)^i}{i!} e^{-\lambda t}, i = 0, 1, 2, \dots, \quad (1)$$

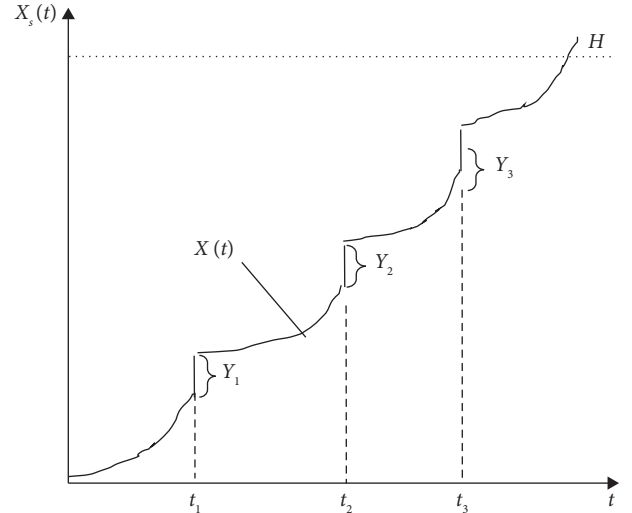


FIGURE 1: Soft failure process.

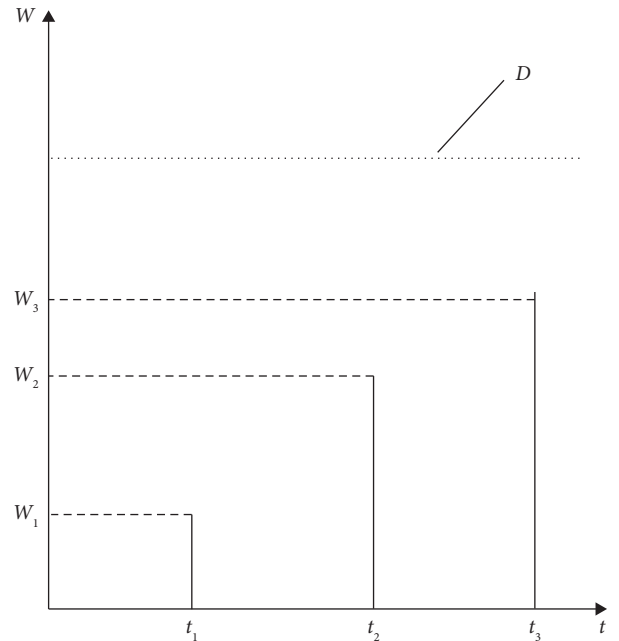


FIGURE 2: Hard failure process.

where, $N(t)$ is the shock number in $(0, t]$

From Figure 2, suppose T is the complex system hard failure time and D is the hard threshold value, under the extreme shock model, we can get

$$P(t \leq T) = P(W_1 < D, W_2 < D, \dots, W_{N(t)} < D). \quad (2)$$

Suppose that magnitudes of the shock $W_i \sim N(\mu_w, \sigma_w^2)$, then we can get

$$P(t \leq T) = \left[\Phi\left(\frac{D - \mu_w}{\sigma_w}\right) \right]^{N(t)}. \quad (3)$$

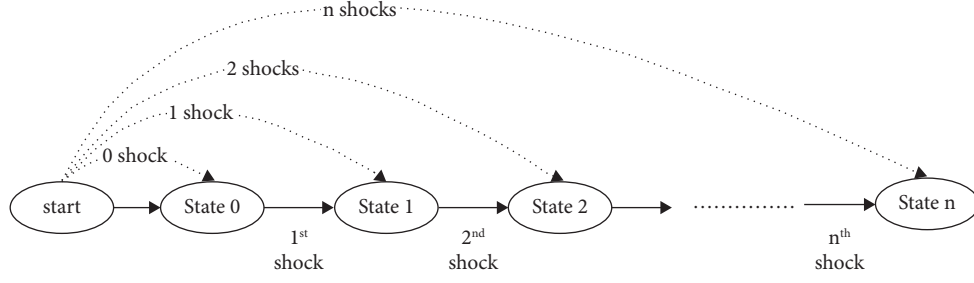


FIGURE 3: State transition charts of the system.

Similarly, under the cumulative shock model, we can get

$$P(t \leq T) = P(W_1 + W_2 + \dots + W_{N(t)} < D). \quad (4)$$

And we can get

$$P(t \leq T) = \left[\Phi \left(\frac{D - N(t)\mu_w}{\sqrt{N(t)}\sigma_w} \right) \right]. \quad (5)$$

3.2. Degradation Process Analysis. Considering that the dynamics characterizes the random uncertainty, the non-linearity, the uncertainty of measurement, and individual differences exist extensively in the practice degradation process, a general nonlinearity random effect. Wiener process with measurement error model M_0 is expressed as follows:

$$\begin{cases} X(t) = X(0) + \beta\Lambda(t, \gamma_1) + \sigma_B B(\Lambda(t, \gamma_2)) + \varepsilon, \\ \beta \sim N(\mu_\beta, \sigma_\beta^2), \end{cases} \quad (6)$$

where, the initial value $X(0)$ is a constant, the $\Lambda(t, \gamma_1)$ and $\Lambda(t, \gamma_2)$ are the time scale, the drift degradation rate β is a random effect parameter, the diffusion coefficient σ_B is the fixed effect parameter, $B(\cdot)$ is the standard Brownian motion, ε is the measurement error and $\varepsilon \sim N(0, \sigma_\varepsilon^2)$. Generally, we suppose $X(0) = 0$; if not, we can use a transform $X'(t) = X(t) - X(0)$.

If $\sigma_\varepsilon = 0$, model M_0 reduces a random effect model M_1 as follows:

$$\begin{cases} X(t) = \beta\Lambda(t, \gamma_1) + \sigma_B B(\Lambda(t, \gamma_2)), \\ \beta \sim N(\mu_\beta, \sigma_\beta^2). \end{cases} \quad (7)$$

If $\sigma_\beta = 0$, the model M_0 reduces a fixed effect model with measurement error M_2 as follows:

$$X(t) = \beta\Lambda(t, \gamma_1) + \sigma_B B(\Lambda(t, \gamma_2)) + \varepsilon. \quad (8)$$

If $\sigma_\beta = 0$ and $\sigma_\varepsilon = 0$, the model M_0 reduces a fixed effect model M_3 as follows:

$$X(t) = \beta\Lambda(t, \gamma_1) + \sigma_B B(\Lambda(t, \gamma_2)). \quad (9)$$

If $\sigma_\beta = 0$, $\sigma_\varepsilon = 0$, and $\gamma_1 = \gamma_2 = \gamma$, the model M_0 reduces a fixed effect model M_4 as follows:

$$X(t) = \beta\Lambda(t, \gamma) + \sigma_B B(\Lambda(t, \gamma)). \quad (10)$$

By using a time-scale transformation, the (10) can be transformed into a linear Wiener process model.

From (6), we can obtain

$$X(t) \sim N(\mu_\beta\Lambda(t, \gamma_1), \sigma_\beta^2(\Lambda(t, \gamma_1))^2 + \sigma_B^2\Lambda(t, \gamma_2) + \sigma_\varepsilon^2). \quad (11)$$

In this section, suppose that each shock load will cause additional abrupt degradation. Let the abrupt degradation be measured sizes as $\{Y_1, Y_2, \dots\}$ and $S(t)$ be the total damage during $(0, t]$, then, we can get

$$S(t) = \begin{cases} \sum_{i=1}^{N(t)} Y_i, & \text{if } N(t) > 0, \\ 0, & \text{if } N(t) = 0. \end{cases} \quad (12)$$

Then, we can obtain

$$X_S(t) = X(t) + S(t). \quad (13)$$

3.3. System Reliability Analysis. We know that the shocks not only can reduce the system performance directly but also can bring a faster degradation rate, resulting in the system's performance level from one state to another. Therefore, we can describe the state transition chart as in Figure 3.

3.3.1. Case I: Extreme Shock Modeling. From the system assumptions, we know that each shock can bring a change in the system state. That is to say, if the i th ($i = 1, 2, \dots, n$) random shock occurs, the system state will divert from state $i - 1$ to state i as the solid line shown in Figure 3. In addition, in the actual arithmetic process, the dotted line expresses the transition path from state 0 to state j in Figure 3.

Therefore, under the extreme shock, the probability at state j can be denoted as follows:

$$\begin{aligned} P_{10} &= P_r(N(t) = 0, X_s(t) < H) = P_r(N(t) = 0, \\ X(t) < H) &= P_r(N(t) = 0)P_r(X(t) < H), \end{aligned} \quad (14)$$

$$\begin{aligned} P_{11} &= P_r(N(t) = 1, X_s(t) < H, W_1 < D) \\ &= P_r(N(t) = 1, X(t) + S(t) < H, W_1 < D) \\ &= P_r(N(t) = 1)P_r(X(t) + Y_1 < H)P_r(W_1 < D), \end{aligned} \quad (15)$$

$$\begin{aligned}
P_{12} &= P_r(N(t) = 2, X_s(t) < H, W_1 < D, W_2 < D) \\
&= P_r(N(t) = 2, X(t) + S(t) < H, W_1 < D, W_2 < D) \\
&= P_r(N(t) = n)P_r(X(t) + Y_1 + Y_2 < H)P_r \\
&\quad (W_1 < D)P_r(W_2 < D),
\end{aligned} \tag{16}$$

$$\begin{aligned}
P_{1n} &= P_r(N(t) = n, X_s(t) < H, W_1 < D, W_2 < D, \\
&\quad \dots, W_n < D,) = P_r(N(t) = n)P_r \\
&\quad (X(t) + Y_1 + Y_2 + \dots + Y_n < H)P_r(W_1 < D) \\
&\quad P_r(W_2 < D) \dots P_r(W_n < D) \\
&= P_r(N(t) = n)P_r\left(X(t) + \sum_{i=1}^{N(t)} Y_i < H\right) \\
&\quad [P_r(W_1 < D)]^{N(t)}.
\end{aligned} \tag{17}$$

Then, the system reliability can be calculated as follows:

$$R = \sum_{i=1}^n P_{1i}. \tag{18}$$

Suppose that Y_i denotes the abrupt damage size with the distribution as follows:

$$Y_i \sim N(\mu_Y, \sigma_Y^2) \quad i = 1, 2, \dots \tag{19}$$

Then, we can get the following:

$$S(t) = \sum_{i=1}^n Y_i \sim N(n\mu_Y, n\sigma_Y^2). \tag{20}$$

By using (11) and (20), we can get the following:

$$\begin{aligned}
X(t) + S(t) &\sim N(\mu_\beta \Lambda(t, \gamma_1) + n\mu_Y, \sigma_\beta^2 (\Lambda(t, \gamma_1))^2 \\
&\quad + \sigma_B^2 \Lambda(t, \gamma_2) + \sigma_\varepsilon^2 + n\sigma_Y^2).
\end{aligned} \tag{21}$$

Then, we can get the following:

$$\begin{aligned}
P_{1n} &= P_r(N(t) = n, X_s(t) < H, W_1 < D, W_2 < D, \dots, \\
&\quad W_n < D,) = P_r(N(t) = n)P_r\left(X(t) + \sum_{i=1}^n Y_i < H\right) \\
[P_r(W_1 < D)]^n &= \frac{\exp(-\lambda t)(\lambda t)^n}{n!}
\end{aligned} \tag{22}$$

$$\begin{aligned}
&\Phi\left(\frac{H - (\mu_\beta \Lambda(t, \gamma_1) + n\mu_Y)}{\sqrt{\sigma_\beta^2 (\Lambda(t, \gamma_1))^2 + \sigma_B^2 \Lambda(t, \gamma_2) + \sigma_\varepsilon^2 + n\sigma_Y^2}}\right) \\
&\left[\Phi\left(\frac{D - \mu_W}{\sigma_W}\right)\right]^n.
\end{aligned}$$

Then, we can get the following:

$$\begin{aligned}
R = \sum_{i=1}^n P_{1i} &= \Phi\left(\frac{H - \mu_\beta \Lambda(t, \gamma_1)}{\sqrt{\sigma_\beta^2 (\Lambda(t, \gamma_1))^2 + \sigma_B^2 \Lambda(t, \gamma_2) + \sigma_\varepsilon^2}}\right) \exp(-\lambda t) + \sum_{i=1}^n \left[\Phi\left(\frac{D - \mu_W}{\sigma_W}\right)\right]^i \\
&\quad \Phi\left(\frac{H - (\mu_\beta \Lambda(t, \gamma_1) + i\mu_Y)}{\sqrt{\sigma_\beta^2 (\Lambda(t, \gamma_1))^2 + \sigma_B^2 \Lambda(t, \gamma_2) + \sigma_\varepsilon^2 + i\sigma_Y^2}}\right) \frac{\exp(-\lambda t)(\lambda t)^i}{i!}.
\end{aligned} \tag{23}$$

3.3.2. Case II: Cumulative Shock Modeling. Similarly, under the cumulative shock, the probability at state j can be denoted as follows:

$$P_{20} = P_r(N(t) = 0, X_s(t) < H) = P_r(N(t) = 0)P_r(X(t) < H), \tag{24}$$

$$\begin{aligned}
P_{21} &= P_r(N(t) = 1, X_s(t) < H, W_1 < D) \\
&= P_r(N(t) = 1, X(t) + Y_1 < H)P_r(W_1 < D) \\
&= P_r(N(t) = n)P_r(X(t) + Y_1 + Y_2 < H)P_r(W_1 + W_2 < D) \\
&= \exp(-\lambda t)(\lambda t)\Phi\left(\frac{H - (\mu_\beta \Lambda(t, \gamma_1) + 2\mu_Y)}{\sqrt{\sigma_\beta^2 (\Lambda(t, \gamma_1))^2 + \sigma_B^2 \Lambda(t, \gamma_2) + \sigma_\varepsilon^2 + 2\sigma_Y^2}}\right) \times \left[\Phi\left(\frac{D - 2\mu_W}{\sqrt{2}\sigma_W}\right)\right],
\end{aligned} \tag{25}$$

$$\begin{aligned}
P_{22} &= P_r(N(t) = 2, X_s(t) < H, W_1 + W_2 < D), \\
&= P_r(N(t) = 2, X(t) + S(t) < H, W_1 + W_2 < D), \\
&= P_r(N(t) = n)P_r(X(t) + Y_1 + Y_2 < H)P_r(W_1 + W_2 < D), \\
&= \frac{\exp(-\lambda t)(\lambda t)^2}{2} \Phi\left(\frac{H - (\mu_\beta \Lambda(t, \gamma_1) + 2\mu_Y)}{\sqrt{\sigma_\beta^2(\Lambda(t, \gamma_1))^2 + \sigma_B^2 \Lambda(t, \gamma_2) + \sigma_\varepsilon^2 + \sigma_Y^2}}\right) \times \left[\Phi\left(\frac{D - 2\mu_W}{\sigma_W}\right)\right],
\end{aligned} \tag{26}$$

$$\begin{aligned}
P_{2n} &= P_r(N(t) = n, X_s(t) < H, W_1 + W_2 + \dots + W_n < D) \\
&= P_r(N(t) = n)P_r(X(t) + Y_1 + Y_2 + \dots + Y_n < H) \cdot P_r(W_1 + W_2 + W_n < D) \\
&= P_r(N(t) = n)P_r\left(X(t) + \sum_{i=1}^{N(t)} Y_i < H\right) \times \left[P_r\left(\sum_{i=1}^{N(t)} W_i < D\right)\right] \\
&= \frac{\exp(-\lambda t)(\lambda t)^n}{n!} \Phi\left(\frac{H - (\mu_\beta \Lambda(t, \gamma_1) + n\mu_Y)}{\sqrt{\sigma_\beta^2(\Lambda(t, \gamma_1))^2 + \sigma_B^2 \Lambda(t, \gamma_2) + \sigma_\varepsilon^2 + n\sigma_Y^2}}\right) \times \left[\Phi\left(\frac{D - i\mu_W}{\sqrt{i} \sigma_W}\right)\right].
\end{aligned} \tag{27}$$

Then, we can get the following:

$$R = \sum_{i=1}^n P_{2i} = \sum_{i=1}^n \frac{\exp(-\lambda t)(\lambda t)^i}{i!} \Phi\left(\frac{H - (\mu_\beta \Lambda(t, \gamma_1) + i\mu_Y)}{\sqrt{\sigma_\beta^2(\Lambda(t, \gamma_1))^2 + \sigma_B^2 \Lambda(t, \gamma_2) + \sigma_\varepsilon^2 + i\sigma_Y^2}}\right) \left[\Phi\left(\frac{D - i\mu_W}{\sqrt{i} \sigma_W}\right)\right]. \tag{28}$$

4. Numerical Example

4.1. An Nonlinear Wiener Process about the Fatigue Crack Growth Data. In this section, fatigue crack growth data sets [23, 25, 26] are used to verify the proposed models and methods. This data set consists of 12 experimental samples, and Table 1 lists all the data set information. In order to verify the proposed model, relevant information about the shock process needs to be given. In this paper, reasonable assumptions are made for the information on the shock process based on real data characteristics and literature.

From Table 1 and Refs [23, 25, 26], we can find the degradation path of the fatigue crack growth, which is nonlinear. Therefore, the nonlinear degradation models can be used to describe the degradation path. In order to use the model $M_0, M_1, M_2, M_3,$ and $M_4,$ we use a transformation $X'(t) = X(t) - 0.9$ to deal with the fatigue crack growth data and let $\Lambda(t) = \Lambda(t, \gamma) = t^\gamma$ in the model $M_0, M_1, M_2, M_3,$ and $M_4.$

We know that the performance of the degradation model depends strongly on the appropriateness of the model describing a product's degradation path. In order to compare the performances of some alternative models, Spiegelhalter et al. [31] proposed the deviance information criterion (DIC) to select the best-fitting model by using the Bayesian approach, and a smaller value of DIC indicates a better model. Based on the models $M_0, M_1, M_2, M_3,$ and $M_4,$ by using the MCMC method, we can get the value of DIC under different models as shown in Table 2.

From Table 2, we can find the model M_0 with the lowest values of DIC, therefore, model M_0 is the best-fitting model. Then, by using the MCMC method, we can get the estimation of unknown parameters under the model M_0 as shown in Table 3.

Then, similarly to Refs [25, 26], we suppose $W_i \sim N(0.06, 0.25), Y_i \sim N(0.04, 0.15), H=2.2, D=2.0,$ and $\lambda=1.0 \times 10^{-5}.$ According to Eqs.(24)–(27), under the cumulative shock, the probability for the component in the

TABLE 1: Fatigue crack growth data from test samples.

Test sample	Cycle/ 10^4												
	0	1	2	3	4	5	6	7	8	9	10	11	12
1	0.90	0.92	0.97	1.01	1.05	1.09	1.15	1.21	1.28	1.36	1.44	1.55	1.72
2	0.90	0.92	0.96	1.00	1.04	1.08	1.13	1.19	1.26	1.34	1.42	1.52	1.67
3	0.90	0.93	0.96	1.00	1.04	1.08	1.13	1.18	1.24	1.31	1.39	1.49	1.65
4	0.90	0.93	0.97	1.00	1.03	1.07	1.10	1.16	1.22	1.29	1.37	1.48	1.64
5	0.90	0.92	0.97	0.99	1.03	1.06	1.10	1.14	1.20	1.26	1.31	1.40	1.52
6	0.90	0.93	0.96	1.00	1.03	1.07	1.12	1.16	1.21	1.27	1.33	1.40	1.49
7	0.90	0.92	0.96	0.99	1.03	1.06	1.10	1.16	1.21	1.27	1.33	1.40	1.49
8	0.90	0.92	0.95	0.97	1.00	1.03	1.07	1.11	1.16	1.22	1.26	1.33	1.40
9	0.90	0.93	0.96	0.97	1.00	1.05	1.08	1.11	1.16	1.20	1.24	1.32	1.38
10	0.90	0.92	0.94	0.97	1.01	1.04	1.07	1.09	1.14	1.19	1.23	1.28	1.35
11	0.90	0.92	0.94	0.97	0.99	1.02	1.05	1.08	1.12	1.16	1.20	1.25	1.31
12	0.90	0.92	0.94	0.97	0.99	1.02	1.05	1.08	1.12	1.16	1.19	1.24	1.29

TABLE 2: Comparison of different models.

Model	M_0	M_1	M_2	M_3	M_4
DIC	-784.3	-779.5	-755.1	-752.9	-733
Ranking	1	2	3	4	5

TABLE 3: Estimation results of the unknown parameters.

Parameter	Mean	Standard error	MC error	95% HPD interval
μ_β	0.020020	0.002668	1.084E-4	(0.014280, 0.02499)
σ_β	0.006386	0.001559	1.667 E-5	(0.004103, 0.01021)
σ_B	0.004968	0.001082	5.871 E-5	(0.003388, 0.00768)
γ_1	1.353000	0.046430	0.002557	(1.278000, 1.47100)
γ_2	2.042000	0.194400	0.010460	(1.620000, 2.38800)
E	6.554 E-9	4.958 E-8	2.988 E-9	(0.0000, 4.818 E-8)

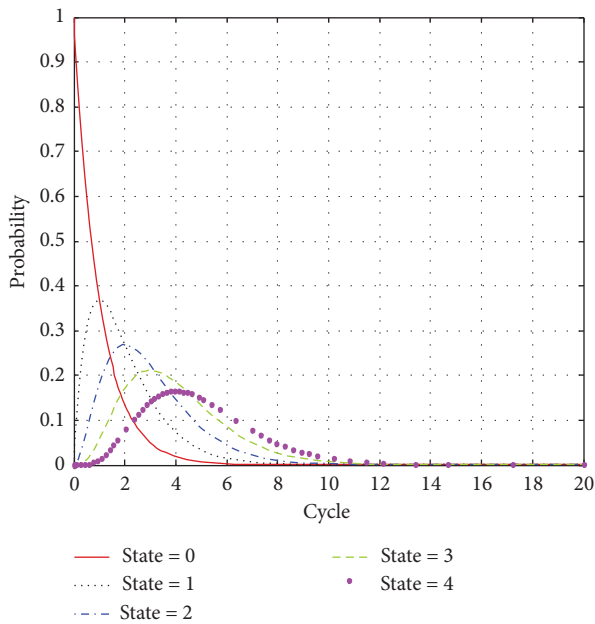


FIGURE 4: Probability curves in different states.

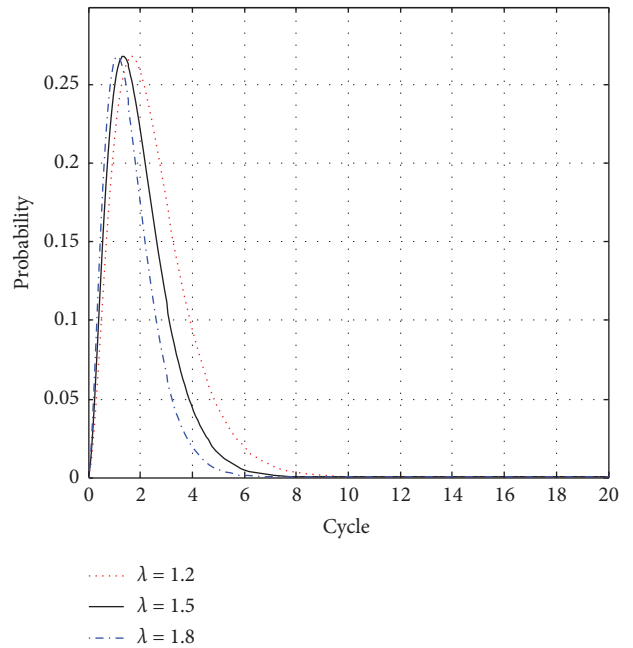


FIGURE 5: Sensitivity analysis of state 2 on λ .

probability of being in state 0, 1, 2, 3, and 4 can be calculated as follows:

$$\begin{aligned}
P_0 &= \exp(-1.0 \times 10^{-5}t) \Phi \left(\frac{H - 0.02002 \times t^{1.353}}{\sqrt{(0.006386 \times t^{1.353})^2 + 0.004986^2 \times t^{2.042} + (6.554 \times 10^{-9})^2}} \right), \\
P_1 &= \exp(-1.0 \times 10^{-5}t) (1.0 \times 10^{-5}t) \left[\Phi \left(\frac{D - 0.06}{0.5} \right) \right] \\
&\quad \times \Phi \left(\frac{H - 0.02002 \times t^{1.353} - 0.04}{\sqrt{(0.006386 \times t^{1.353})^2 + 0.004986^2 \times t^{2.042} + (6.554 \times 10^{-9})^2 + 0.15}} \right), \\
P_2 &= \frac{\exp(-1.0 \times 10^{-5}t) (1.0 \times 10^{-5}t)^2}{2} \left[\Phi \left(\frac{D - 2 \times 0.06}{\sqrt{2} \times 0.5} \right) \right] \\
&\quad \times \Phi \left(\frac{H - 0.02002 \times t^{1.353} - 2 \times 0.04}{\sqrt{(0.006386 \times t^{1.353})^2 + 0.004986^2 \times t^{2.042} + (6.554 \times 10^{-9})^2 + 2 \times 0.15}} \right), \\
P_3 &= \frac{\exp(-1.0 \times 10^{-5}t) (1.0 \times 10^{-5}t)^3}{6} \left[\Phi \left(\frac{D - 3 \times 0.06}{\sqrt{3} \times 0.5} \right) \right] \\
&\quad \times \Phi \left(\frac{H - 0.02002 \times t^{1.353} - 3 \times 0.04}{\sqrt{(0.006386 \times t^{1.353})^2 + 0.004986^2 \times t^{2.042} + (6.554 \times 10^{-9})^2 + 3 \times 0.15}} \right), \\
P_4 &= \frac{\exp(-1.0 \times 10^{-5}t) (1.0 \times 10^{-5}t)^4}{24} \left[\Phi \left(\frac{D - 4 \times 0.06}{\sqrt{4} \times 0.5} \right) \right] \\
&\quad \times \Phi \left(\frac{H - 0.02002 \times t^{1.353} - 4 \times 0.04}{\sqrt{(0.006386 \times t^{1.353})^2 + 0.004986^2 \times t^{2.042} + (6.554 \times 10^{-9})^2 + 4 \times 0.15}} \right).
\end{aligned} \tag{29}$$

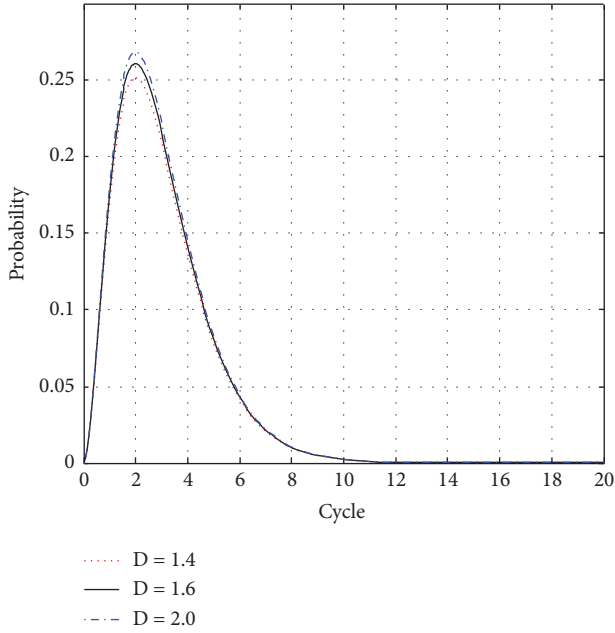
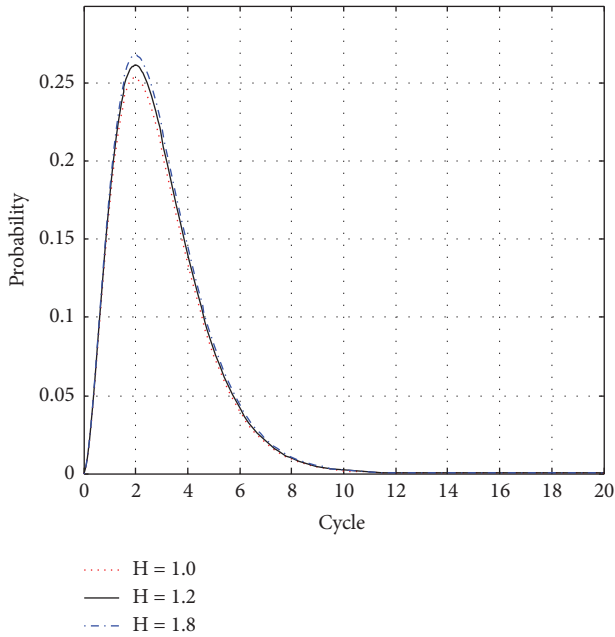
If we let the vertical axis denote the probability of the system performance, and the horizontal axis denotes time. Then, Figure 4 shows the probability curve in every state i ($i=0, 1, 2, 3, 4$) as a function of time t . From Figure 4, we know that when the system reaches state 2, the probability of the system performance is approximately 0.26 at 2×10^4 cycle. Moreover, with the increase of time and the number of shocks, we can find the probabilities of the system performance gradually decreasing.

In order to analyze the probability of the system performance better in the different states, the sensitivity analysis method is used in this paper. Take state 2 as an example, the sensitivity analysis about the different parameters is plotted in Figures 5–7. From Figures 5–7, we can find that the failure threshold H (or D) and the arrivals rate λ of random shocks all have an important effect on the probability of the system performance.

In addition, based on (27), the system reliability can be obtained as follows:

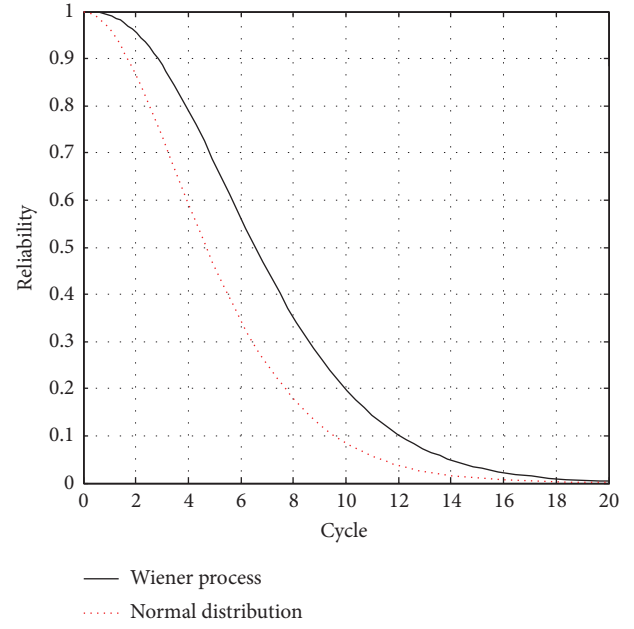
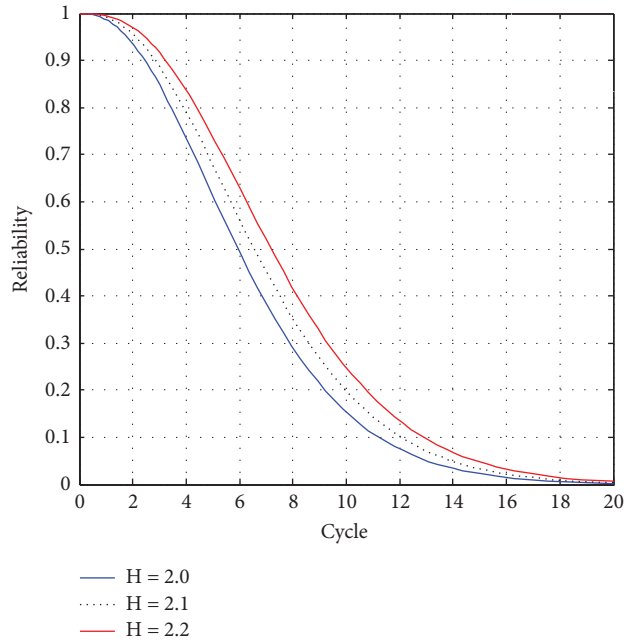
$$\begin{aligned}
R &= \sum_{i=1}^n P_i = \Phi \left(\frac{H - 0.01835 \times t^{1.396}}{\sqrt{(0.00639 \times t^{1.396})^2 + 0.00641^2 \times t^{1.851}}} \right) \\
&\quad \cdot \exp(-1.0 \times 10^{-5}t) + \sum_{i=1}^n \left[\Phi \left(\frac{D - 0.06}{0.5} \right) \right]^i \\
&\quad \cdot \Phi \left(\frac{H - 0.01476 \times t^{1.491} - i \times 0.04}{\sqrt{(0.00639 \times t^{1.396})^2 + 0.00641^2 \times t^{1.851} + i \times 0.15}} \right) \\
&\quad \times \frac{\exp(-1.0 \times 10^{-5}t) (-1.0 \times 10^{-5}t)^i}{i!}.
\end{aligned} \tag{30}$$

Similarly, according to the parameter estimation results in Table 3, the solid curve of the system reliability $R(t)$ based on the nonlinear random effect Wiener process is plotted in Figure 8. From Figure 8, we can find that the reliability of the

FIGURE 6: Sensitivity analysis of $(P)_2$ on (D) .FIGURE 7: Sensitivity analysis of $(P)_2$ on (H) .

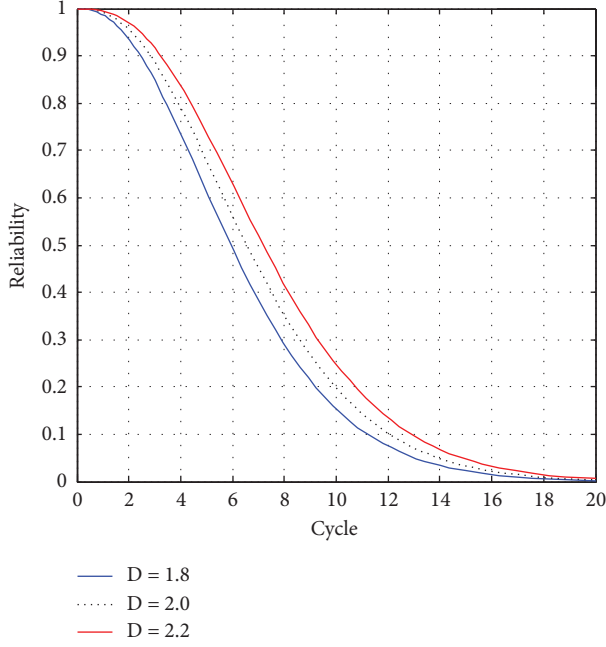
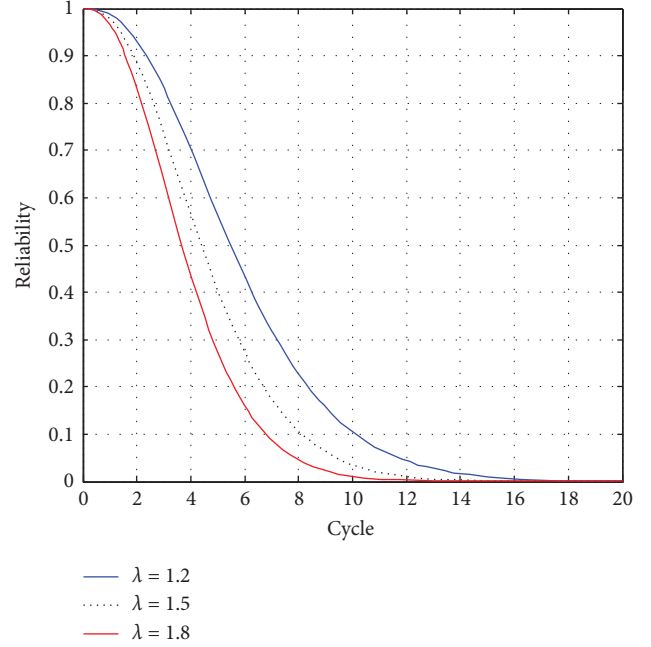
system almost keeps 1 when $t < 0.8 \times 10^4$ cycles, and when $t > 0.8 \times 10^4$ cycles, the reliability decline rapidly. The dotted curve of the system reliability $R(t)$ based on the normal process in Ref [25] is also plotted in Figure 8. Compared with two different degradation models, the normal process assumption underestimates the system's reliability.

The sensitivity analysis for the system reliability $R(t)$ based on the nonlinear random effect Wiener process about the different parameters is plotted in Figures 9–11. From Figures 9–11, we can find that the failure threshold H (or D) and the arrivals rate λ of random shocks all have an

FIGURE 8: The curve of system reliability $R(t)$.FIGURE 9: Sensitivity analysis of $R(t)$ on H .

important effect on the probability of the system performance. We can also find that the reliability curves shift to the left when the shock arrival rate λ increases from 1.2 to 1.8, but the reliability curves shift to the right when the failure threshold H increases from 2.0 to 2.2 or D increases from 1.8 to 1.2.

4.2. A Real Example of MEMS Oscillators. A MEMS oscillator is a time device and is widely used in electronic systems, transfer systems, and measure systems. The

FIGURE 10: Sensitivity analysis of $R(t)$ on D .FIGURE 11: Sensitivity analysis of $R(t)$ on λ .

electronic system is a typical system which is subjected to both mechanical and voltage shocks. As we know, on account of operating losses, the mass of MEMS oscillators will decrease over time, and the loss of mass can increase the frequency of vibration. In this paper, similarly to Ref [32, 33], we use a fixed effect Wiener process M_4 as shown in (10) to describe the nature process and use the Poisson process in (1) to describe the shock process. The parameters of the Wiener process and Poisson shock process are shown in Table 4.

Similarly, according to Eqs.(14)–(17), under the extreme shock, the probability of the component in the probability of being in state 0, 1, 2, 3, and 4 can be calculated as follows:

$$\begin{aligned}
 P_0 &= \exp(-0.013t) \Phi\left(\frac{H-0.9 \times t}{\sqrt{20^2 \times t}}\right), \\
 P_1 &= \exp(-0.013t) (0.013t) \Phi\left(\frac{H-0.9 \times t - 400}{\sqrt{20^2 \times t + 15^2}}\right) \left[\Phi\left(\frac{D-72.6}{6.3}\right)\right], \\
 P_2 &= \frac{\exp(-0.013t) (0.013t)^2}{2} \Phi\left(\frac{H-0.9 \times t - 2 \times 400}{\sqrt{20^2 \times t + 2 \times 15^2}}\right) \left[\Phi\left(\frac{D-72.6}{6.3}\right)\right]^2, \\
 P_3 &= \frac{\exp(-0.013t) (0.013t)^3}{6} \Phi\left(\frac{H-0.9 \times t - 3 \times 400}{\sqrt{20^2 \times t + 3 \times 15^2}}\right) \left[\Phi\left(\frac{D-72.6}{6.3}\right)\right]^3, \\
 P_4 &= \frac{\exp(-0.013t) (0.013t)^4}{24} \Phi\left(\frac{H-0.9 \times t - 4 \times 400}{\sqrt{20^2 \times t + 4 \times 15^2}}\right) \left[\Phi\left(\frac{D-72.6}{6.3}\right)\right]^4.
 \end{aligned} \tag{31}$$

Figure 12 shows the probability curve of MEMS oscillator in every state i ($i = 0, 1, 2, 3, 4$) as a function of time t . From Figure 12, we know that when the system reaches state 4, the probability of the system performance is

TABLE 4: Parameter values of the Wiener process and Poisson process.

Parameter	Values	Sources
H	4100	Ref [32, 33]
D	92	Ref [32, 33]
Λ	0.013	Ref [32, 33]
M	0.9	Ref [32, 33]
Σ	20	Ref [32, 33]
μ_W	72.6	Ref [32, 33]
σ_W	6.3	Ref [32, 33]
μ_Y	400	Ref [32, 33]
σ_Y	15	Ref [32, 33]
$\gamma_1 = \gamma_2$	1.0	Ref [32, 33]

approximately 0.195 at 300 months. Take state 4 as an example, the sensitivity analysis about the different parameters is plotted in Figures 13–15. From Figures 13–15, we can find that the failure threshold H (or D) and the arrivals rate λ of random shocks all have an important effect on the probability of the system performance.

Then, based on (23), the reliability of the system which is the total probability of different states can be obtained as follows:

$$\begin{aligned}
 R &= \sum_{i=1}^{N(t)} P_i = \Phi\left(\frac{H-0.9 \times t}{\sqrt{20^2 \times t}}\right) \exp(-0.013t) \\
 &+ \sum_{i=1}^m \left[\Phi\left(\frac{D-72.6}{6.3}\right)\right]^i \Phi\left(\frac{H-0.9 \times t - 3 \times 400}{\sqrt{20^2 \times t + 3 \times 15^2}}\right) \\
 &\times \frac{\exp(-1.0 \times 10^{-5}t) (-1.0 \times 10^{-5}t)^j}{j!}.
 \end{aligned} \tag{32}$$

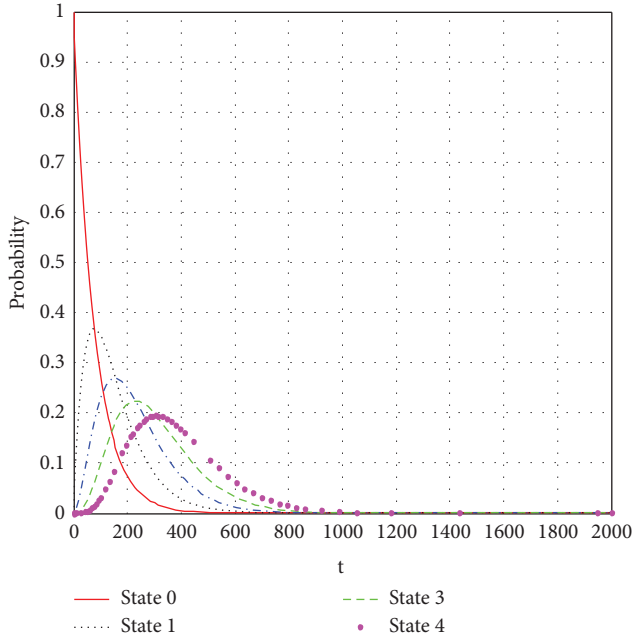


FIGURE 12: Probability curves in different states.

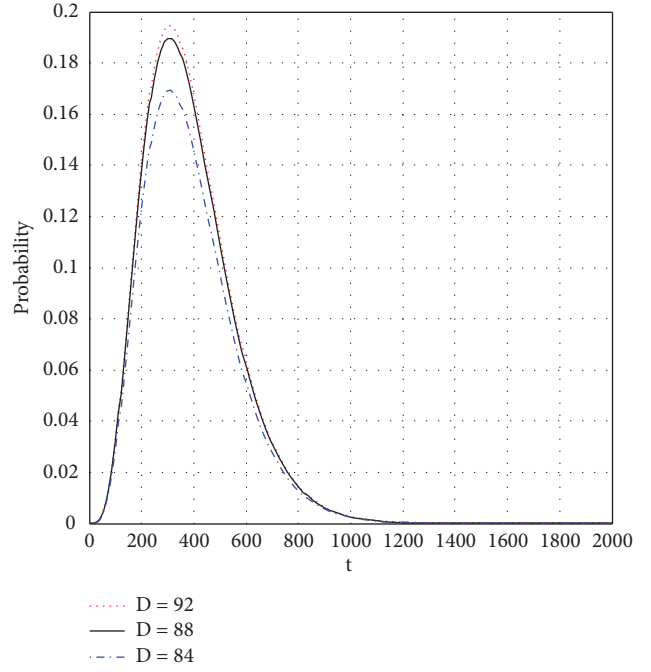


FIGURE 14: Sensitivity analysis of $(P)_4$ on (D) .

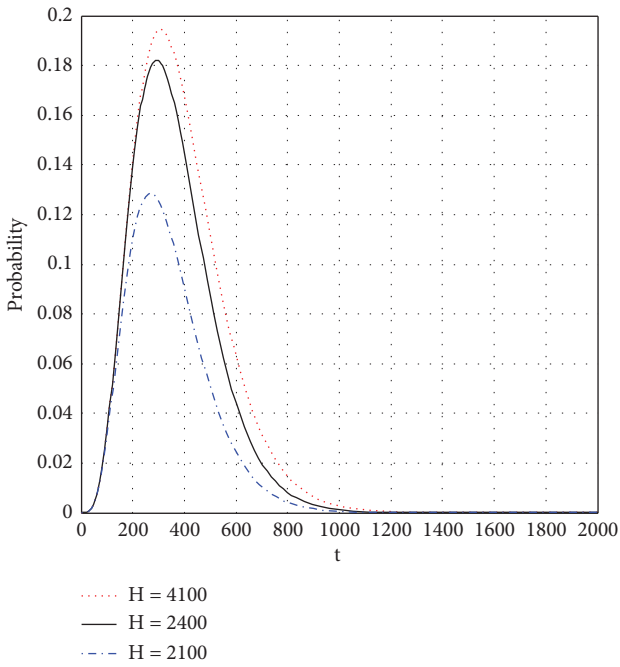


FIGURE 13: Sensitivity analysis of $(P)_4$ on (H) .

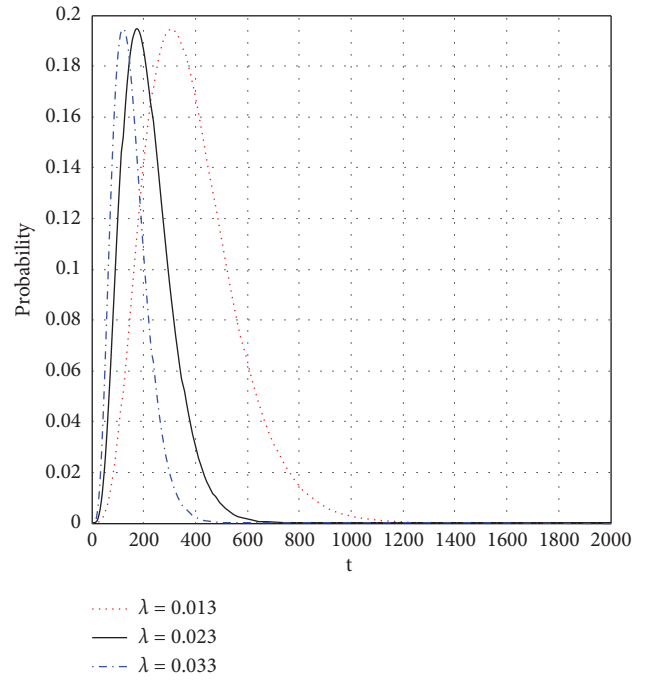


FIGURE 15: Sensitivity analysis of $(P)_4$ on λ .

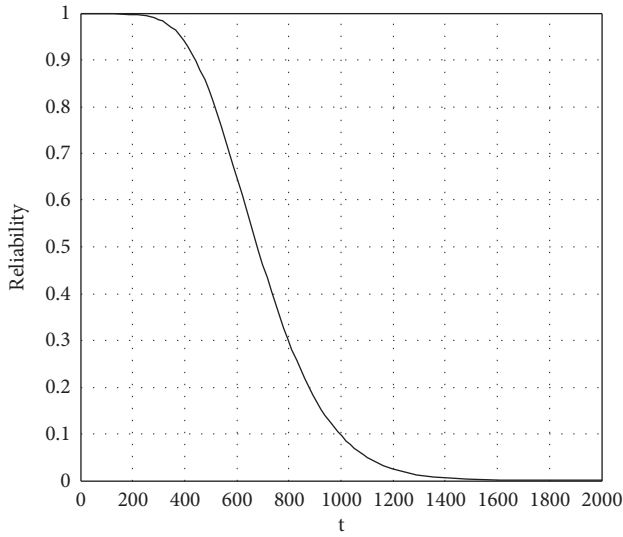


FIGURE 16: The curve of the system reliability $R(t)$.

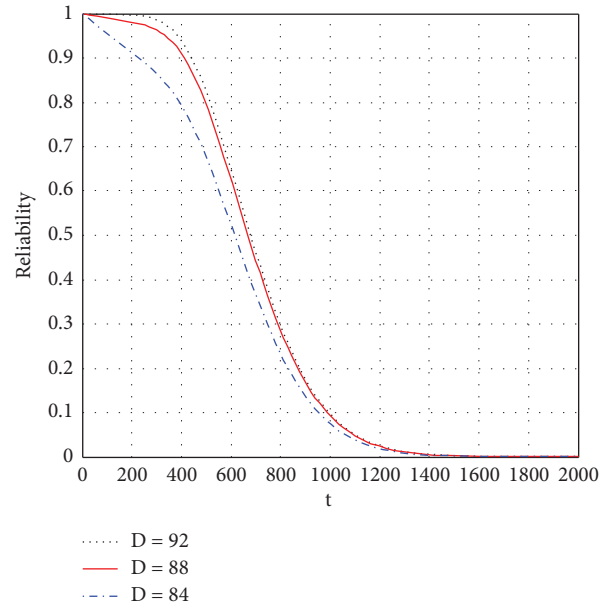


FIGURE 18: Sensitivity analysis of $R(t)$ on D .

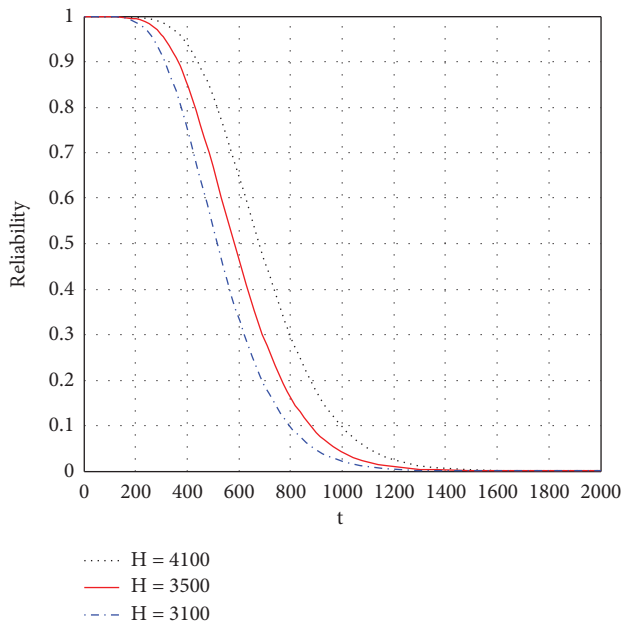


FIGURE 17: Sensitivity analysis of $R(t)$ on H .

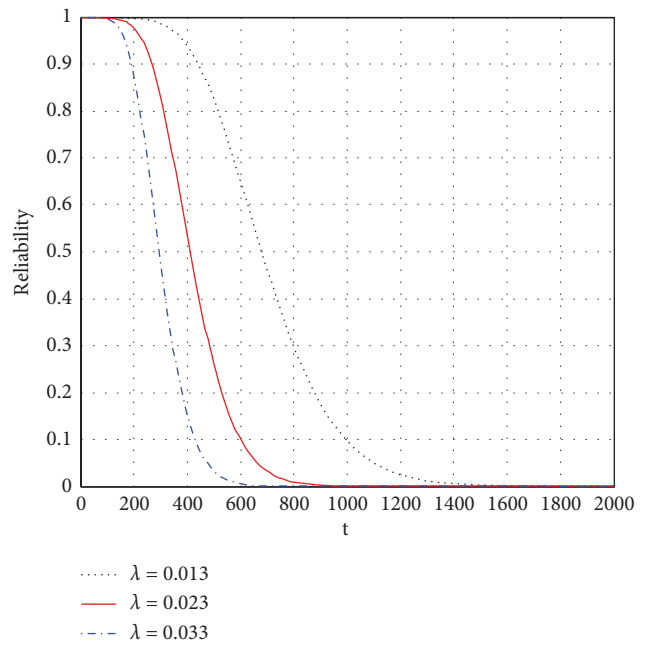


FIGURE 19: Sensitivity analysis of $R(t)$ on λ .

Similarly, the curve of the system reliability $R(t)$ is plotted in Figure 16 by using the estimation results in Table 4. From Figure 16, we can find that the reliability of the system almost keeps 1 when $t < 230$ months, and when $t > 230$ months, the reliability declines rapidly. The sensitivity analyses about the different parameters are plotted in Figures 17–19. From Figures 17–19, we can find that the reliability curves shift to the right when parameter H increases from 3100 to 4100 or D increases from 84 to 92, but the reliability curves shift to the left when the shock arrival rate λ increases from 0.013 to 0.033.

5. Conclusions

This paper studied a multi-state complex degradation system reliability assessment model suffering from the DCFP model with nonlinear random effect Wiener process with measurement error and random shocks. Different from the traditional multi-state system model, the transmission time from state i to $i+1$ is a random variable. By using the multi-state system reliability theory, the system state probabilities are obtained under the different degradation state points, and then the system reliability is obtained. Two

numerical examples of fatigue crack growth and MEMS oscillators are given to illustrate the model and method. By analyzing the influence of different parameters on the state probability and the system reliability, some sensitivity analyses are obtained. In future research, some other stochastic processes and shock models are worth investigating.

Data Availability

The data used to support the findings of this study are available from the corresponding author upon request.

Conflicts of Interest

The authors declare that they have no conflicts of interest regarding the publication of this article.

Authors' Contributions

The authors contributed equally to the presented mathematical framework and the writing of the paper. All authors have read and approved the final manuscript.

Acknowledgments

This work was supported by the Humanity and Social Science Foundation of Ministry of Education of China (No. 19YJAZH039), the Technology Creative Project of Excellent Middle & Young Team of Hubei Province (T201920), the Research Foundation for Advanced Talents of Suqian University (106-CK00042/059), and the Humanity and Social Science Foundation of Ministry of Education of China (No. 20YJAZH035).

References

- [1] A. Lianianski and G. Levitin, *Multi-State System Reliability: Assessment, Optimization and Applications*, World Scientific, New York, NY, USA, 2003.
- [2] G. Levitin, "Block diagram method for analyzing multi-state systems with uncovered failures," *Reliability Engineering & System Safety*, vol. 92, no. 6, pp. 727–734, 2007.
- [3] J. Yu, S. Zheng, H. Pham, and T. Chen, "Reliability modeling of multi-state degraded repairable systems and its applications to automotive systems," *Quality and Reliability Engineering International*, vol. 34, no. 3, pp. 459–474, 2018.
- [4] O. Chryssaphinou, N. Limnios, and S. Malefaki, "Multi-state reliability systems under discrete time semi-Markovian hypothesis," *IEEE Transactions on Reliability*, vol. 60, no. 1, pp. 80–87, 2011.
- [5] I. W. Soro, M. Nourelfath, and D. Ait-Kadi, "Performance evaluation of multi-state degraded systems with minimal repairs and imperfect preventive maintenance," *Reliability Engineering & System Safety*, vol. 95, no. 2, pp. 65–69, 2010.
- [6] M. Compare, P. Baraldi, I. Bani, E. Zio, and D. Mc Donnell, "Development of a Bayesian multi-state degradation model for up-to-date reliability estimations of working industrial components," *Reliability Engineering & System Safety*, vol. 166, pp. 25–40, 2017.
- [7] G. Levitin, H. P. Jia, Y. Ding, Y. Song, and Y. Dai, "Reliability of multi-state systems with free access to repairable standby elements," *Reliability Engineering & System Safety*, vol. 167, pp. 192–197, 2017.
- [8] M. Nourelfath, E. Châtelet, and N. Nahas, "Joint redundancy and imperfect preventive maintenance optimization for series-parallel multi-state degraded systems," *Reliability Engineering & System Safety*, vol. 103, pp. 51–60, 2012.
- [9] C. Fang and L. Cui, "Balanced systems by considering multi-state competing risks under degradation processes," *Reliability Engineering & System Safety*, vol. 205, Article ID 107252, 2021.
- [10] W. Li and H. Pham, "An inspection-maintenance model for systems with multiple competing processes," *IEEE Transactions on Reliability*, vol. 54, no. 2, pp. 318–327, 2005.
- [11] S. Eryilmaz, "Assessment of a multi-state system under a shock model," *Applied Mathematics and Computation*, vol. 269, pp. 1–8, 2015.
- [12] M. C. Segovia and P. E. Labeau, "Reliability of a multi-state system subject to shocks using phase-type distributions," *Applied Mathematical Modelling*, vol. 37, no. 7, pp. 4883–4904, 2013.
- [13] W. Li and H. Pham, "Reliability modeling of multi-state degraded systems with multi-competing failures and random shocks," *IEEE Transactions on Reliability*, vol. 54, no. 2, pp. 297–303, 2005.
- [14] Y. H. Lin, Y. F. Li, E. Zio, Y. F. Li, and E. Zio, "Integrating random shocks into multi-state physics models of degradation processes for component reliability assessment," *IEEE Transactions on Reliability*, vol. 64, no. 1, pp. 154–166, 2015.
- [15] H. Pham, A. Suprasad, and R. B. Misra, "Availability and mean life time prediction of multistage degraded system with partial repairs," *Reliability Engineering & System Safety*, vol. 56, no. 2, pp. 169–173, 1997.
- [16] Y. Wang and H. Pham, "A multi-objective optimization of imperfect preventive maintenance policy for dependent competing risk systems with hidden failure," *IEEE Transactions on Reliability*, vol. 60, no. 4, pp. 770–781, 2011.
- [17] Y. Wang and H. Pham, "Imperfect preventive maintenance policies for two-process cumulative damage model of degradation and random shocks," *International Journal of System Assurance Engineering and Management*, vol. 2, no. 1, pp. 66–77, 2011.
- [18] Y. Wang and H. Pham, "Modeling the dependent competing risks with multiple degradation processes and random shock using time-varying copulas," *IEEE Transactions on Reliability*, vol. 61, no. 1, pp. 13–22, 2012.
- [19] R. Wang and M. Zhu, "Shock-loading-based reliability modeling with dependent degradation processes and random shocks," *International Journal of Reliability, Quality and Safety Engineering*, vol. 29, no. 03, 2022.
- [20] M. Park and H. Pham, "Condition-based maintenance for a degradation-shock dependence system under warranty," *International Journal of Production Research*, vol. 2022, pp. 1–16, 2022.
- [21] H. Peng, Q. Feng, and D. W. Coit, "Reliability and maintenance modeling for systems subject to multiple dependent competing failure processes," *IIE Transactions*, vol. 43, no. 1, pp. 12–22, 2010.
- [22] L. Jiang, Q. Feng, and D. W. Coit, "Reliability and maintenance modeling for dependent competing failure processes with shifting failure thresholds," *IEEE Transactions on Reliability*, vol. 61, no. 4, pp. 932–948, 2012.
- [23] Z. Wang, H. Z. Huang, and L. Du, "Reliability analysis on competitive failure processes under fuzzy degradation data," *Applied Soft Computing*, vol. 11, no. 3, pp. 2964–2973, 2011.

- [24] A. Jiang, L. Huang, and Y. Xiang, "Reliability analysis for competitive failure processes with multi-state degradation," in *Proceedings of the IEEE Asia-Pacific International Symposium on Advanced Reliability and Maintenance Modeling (APARM)*, pp. 1–7, Vancouver, BC, Canada, August 2020.
- [25] H. Li, R. Yuan, and J. Fu, "A reliability modeling for multi-component systems considering random shocks and multi-state degradation," *IEEE Access*, vol. 7, pp. 168805–168814, 2019.
- [26] Z. Wang, H. Z. Huang, Y. Li, and N. C. Xiao, "An approach to reliability assessment under degradation and shock process," *IEEE Transactions on Reliability*, vol. 60, no. 4, pp. 852–863, 2011.
- [27] X. S. Si, W. B. Wang, C. H. Hu, D. H. Zhou, and M. G. Pecht, "Remaining useful life estimation based on a nonlinear diffusion degradation process," *IEEE Transactions on Reliability*, vol. 61, no. 1, pp. 50–67, 2012.
- [28] D. B. Meng, S. Y. Yang, C. He et al., "Multidisciplinary design optimization of engineering systems under uncertainty: a review," *International Journal of Structural Integrity*, vol. 13, no. 4, pp. 565–593, 2022.
- [29] D. B. Meng, T. W. Xie, P. Wu, S. P. Zhu, Z. Hu, and Y. Li, "Uncertainty-based design and optimization using first order saddlepoint approximation method for multidisciplinary engineering systems," *ASCE-ASME Journal of Risk and Uncertainty in Engineering Systems, Part A: Civil Engineering*, vol. 6, no. 3, pp. 1–8, 2020.
- [30] D. B. Meng, H. T. Wang, S. Y. Yang, Z. Lv, Z. Hu, and Z. Wang, "Fault analysis of wind power rolling bearing based on EMD feature extraction," *Computer Modeling in Engineering and Sciences*, vol. 130, no. 1, pp. 543–558, 2022.
- [31] D. J. Spiegelhalter, N. G. Best, B. P. Carlin, and A. Van Der Linde, "Bayesian measures of model complexity and fit," *Journal of the Royal Statistical Society: Series B*, vol. 64, no. 4, pp. 583–639, 2002.
- [32] S. Song, D. W. Coit, and Q. Feng, "Reliability for systems of degrading components with distinct component shock sets," *Reliability Engineering & System Safety*, vol. 132, pp. 115–124, 2014.
- [33] F. Sun, H. Li, Y. Cheng, and H. Liao, "Reliability analysis for a system experiencing dependent degradation processes and random shocks based on a nonlinear Wiener process model," *Reliability Engineering & System Safety*, vol. 215, 2021.